Comparative Analysis of Resistive Dipole Accelerator Magnets for a Muon Collider

Comparative analysis of resistive dipole accelerator magnets for a Muon Collider

M. Breschi, *Senior Member, IEEE,* L. Cavallucci, R. Miceli, P. L. Ribani, L. Bottura, F. Boattini, S. Fabbri, H. De Gersem

***Abstract*— This work focuses on the design of resistive dipole accelerator magnets for the Muon Collider accelerator under study in the frame of the International Muon Collider Cooperation (IMCC) and with the participation of the European Union (MuCol program). The design specifications require that these dipoles are subjected to very fast ramps, with ramp times in the range from 1 ms to 10 ms. This in turn results in the need for very high power, in the order of tens of GWs for the chain of Rapid Cycling Synchrotrons (RCS) to be realized. For the magnet design, three geometric configurations were considered and compared in this study, namely the hourglass magnet (previously considered in the US Muon Collider design study), the windowframe magnet and the H-type magnet. An optimization procedure was carried out to minimize the energy stored in the magnet, in order to reduce the energizing power during the fast ramps. The results found for the three considered configurations at different current densities are compared in the paper in terms of total stored energy, total losses during the operation current cycle and field quality. The H-type magnet is identified as a suitable configuration due to both low stored energy and low losses.**

***Index Terms* —Resistive magnets, Accelerator magnets, Muon Collider, Design optimization.**

I. Introduction

THE accelerator under study within the scope of the EU efforts towards a Muon Collider, will rely on fast acceleration of the decaying muon beams to overcome the short life of 2.2 μs at rest, profiting from nearly five orders of magnitude relativistic time dilation at the final energy of 5 TeV [1-3]. To achieve this, the baseline acceleration scheme foresees the use of a chain of Rapid Cycling Synchrotrons (RCS) with ramp times in the range of 1 ms to 10 ms. The RCS main dipole magnet system is among the main challenges of one such accelerator. The main specifications of the resistive dipole magnets call for a magnetic field in the 30 mm x 100 mm rectangular aperture of 1.8 T, ramped in 1 ms, and homogeneity in the range of few 10^{-4}. The aim of the analysis is twofold: on the one hand it is necessary to limit the magnet stored energy, as this allows one limiting the power required from the power supply during fast ramps. On the other hand, the design should minimize the losses during electrodynamic transients in the copper coils and in the ferromagnetic yoke of the magnet to reduce power consumption.

To this purpose, three geometric configurations were considered and compared in this study, namely the hourglass magnet (previously considered in the US Muon Collider design study [4]), the windowframe magnet [5] and the H-type magnet [5, 6]. An optimization procedure was developed to minimize the energy stored in the magnet and the total losses. This procedure was applied to design the magnets setting the peak engineering current density in the coils to different values ranging from 10 to 30 A/mm^2. All optimized configurations obtained reach the desired magnetic field in the gap, which is set as a constraint of the procedure. The results found for the three configurations at different current densities are compared in the paper in terms of total stored energy, total losses during the operation current cycle and field quality.

II. Design Procedure

A. Design specifications

The resistive dipole magnets to be designed for the Muon Collider accelerator are characterized by the following main specifications:

1) Magnetic field in the aperture of 1.8 T
2) Magnetic field homogeneity within 10×10^{-4} in the good field region (30 mm × 100 mm)
3) Ramps from $-B_{\max}$ to $+B_{\max}$ in 1 ms. The objective for the value of $B_{\max}$ is 2.0 T
4) Limit the magnetic stored energy (crucial design specification to limit the supplied power)
5) Limit the total losses (iron + copper).

B. Design methodology

The design of the resistive magnets is obtained by solving the following constrained optimization problem:

$$\begin{gathered}\min F(\boldsymbol{x}) \\ \boldsymbol{x}_{\min} \le \boldsymbol{x} \le \boldsymbol{x}_{\max} \\ \boldsymbol{G}(\boldsymbol{x}) \le 0\end{gathered} \tag{1}$$

where $\boldsymbol{x}$ is the vector of geometrical variables which define the magnet geometry, $F(\boldsymbol{x})$ is the function to be minimized, $\boldsymbol{x}_{min}$

The work at Università di Bologna was performed in the frame of the Muon Collider EU Design study *(Corresponding author: Marco Breschi).*

M. Breschi, L. Cavallucci, R. Miceli, and P. L. Ribani are with the Department of Electrical, Electronic and Information Engineering, Università di Bologna, Italy (e-mail: marco.breschi@unibo.it).

L. Bottura, F. Boattini and S. Fabbri are with CERN, Geneva, Switzerland.
H. De Gersem is with the Technische Universität Darmstadt, Germany.

and $\boldsymbol{x}_{max}$ the lower and upper bounds of each variable respectively. The function to be minimized is the total magnetic energy of the magnet in DC simulations, or the active, reactive, apparent power in AC simulations.

Finally, G($\boldsymbol{x}$) is a nonlinear constraint, which is adopted to fulfil the design specification concerning the field in the dipole aperture. The *y*-component of the magnetic flux density in the centre of the free gap $B_{0,y}$ (x) should be greater than the reference value: $B_{0,y}(x) - B_{yref} \geq 0$ (B_{yref} = 1.8 T). During the process of minimization of the energy, the field decreases as much as possible, but cannot become lower than the reference value.

C. Minimization problem solution

The problem is solved by means of the routine *fmincon* in a Matlab environment [7]. Three possible optimization algorithms can be used to perform computations, namely SQP (Sequential Quadratic Programming), Interior-point and Active-set [8].

The magnetic energy (objective function) and the magnetic flux density in the centre of the free gap are calculated by means of a two-dimensional FEM model of the magnet implemented in the FEMM software [9].

The problem is solved either in DC conditions or AC conditions during the optimization process. The FEMM model is called at each iteration by the Matlab optimization routine and returns the values of the magnetic field in the centre of the air gap of the magnet and of the total magnetic energy of the magnet. To compare the different configurations analyzed, the homogeneity of the magnetic field in the free gap is evaluated by means of the following parameter δ_B:

$$\delta_B = \frac{\sqrt{\frac{1}{A_{\text{gap}}}\iint_{A_{gap}}\left[\left(B_x - B_{xref}\right)^2 + \left(B_y - B_{yref}\right)^2\right]dx\,dy}}{B_{yref}} \qquad (2)$$

where A_{gap} is the cross section of the free gap (100 mm × 30 mm). The objective is that the *x* component of the magnetic flux density, B_x, should be as small as possible: B_{xref} = 0 T.

D. Design current cycle

In the first 2 ms of each operation cycle (100 ms), it is assumed that the current varies as a sinus with a period of 2 ms. In the remaining 98 ms it remains constant at 0 kA (see Fig. 1).

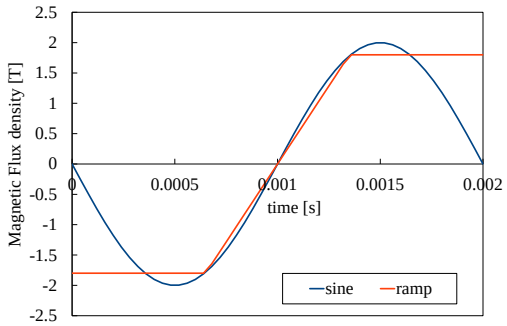

Fig. 1. Reference magnetic cycle ramp, and sinusoidal approximation.

To obtain a ramp from −1.8 T to +1.8 T, the field is approximated with a sinusoid having a peak of 2 T.

E. FEMM model assumptions in DC regime

Two commercial ferromagnetic materials were selected for the magnetic circuit of the resistive dipole. Supermendur is used for the poles of the magnetic circuit, while M22 steel is used for the rest of the ferromagnetic yoke. The non-linear characteristics of the two materials are shown in Fig. 2. It is worth noting that Supermendur guarantees a high value of the magnetic permeability up to the design field of 2.0 T, which is very useful to limit the number of Ampere-turns and thus the Joule losses due to transport current in the conductor. Moreover, the linear behavior of the magnetic characteristics reduces the iron losses during the fast electrodynamic transients. Unfortunately, Supermendur contains Cobalt, which can be activated in presence of radiation; this issue is presently under investigation. On the other hand, M22 steel is cheaper, insensitive to radiation and, notwithstanding its lower saturation field, can be effectively adopted for the lateral branches of the ferromagnetic yoke, where the magnetic flux density is lower.

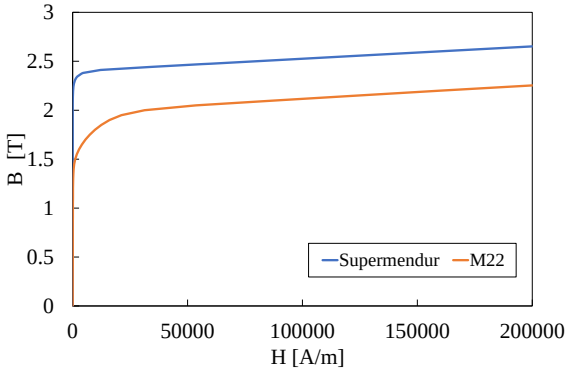

Fig. 2. Non-linear characteristics of the two ferromagnetic materials adopted for the magnetic poles (Supermendur) and the iron yoke (M22) [9].

F. FEMM model assumptions in AC regime

To estimate the losses in one cycle of operation, an AC regime with 500 Hz frequency (period of 2 ms) is considered in FEMM. The losses over one cycle are calculated accounting for transport current, skin effect, proximity effect in the copper, and for hysteresis and eddy current losses in the iron. The non-linear characteristics of the ferromagnetic materials are linearized and a hysteresis lag θ is considered between the phasors of H and B.

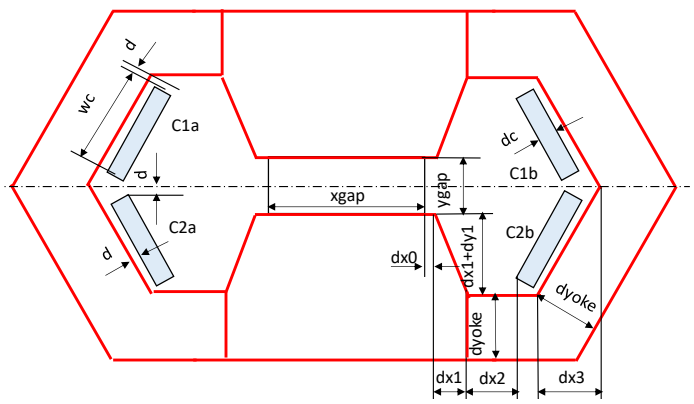

Fig. 3. Hourglass (HG) magnet geometry.

The lag θ is computed by fitting with a dedicated FEMM model experimental data on hysteresis losses measured on a toroidal sample. For Supermendur a hysteresis loss of 236 J/(m^3 cycle) is considered for a cycle with B_{max} = 2 T [10]. For M22 steel a total loss of 520 J/(m3 cycle) is considered for a cycle at 60 Hz and B_{max} = 1.5 T [11]. The difference between the frequency of 60 Hz and that of the magnet operation gives some uncertainty on the values of iron losses. Since the objective of this work is a comparative study of selected configurations, this uncertainty does not affect the conclusions of the analysis.

G. Geometric variables for the optimization

The geometry of the hourglass magnet is presented in Fig. 3. For this magnet, the geometric parameters kept constant and those varied during the optimization are illustrated as an example. In particular, the following values were optimized: dx_1, dx_2, dx_3, dy_1, d_{yoke} and χ (d_c/wc). The geometric parameters kept constant during the optimization process are the following: x_{gap}, y_{gap}, dx_0 and d. It should be noted that x_{gap} and y_{gap} define the gap region and are thus set by the design specifications to 100 mm and 30 mm respectively. The value of d is kept to a minimum of 3 mm to allow for the insulation of the conductor. The distance dx_0 represents the additional width of the magnetic pole, with respect to the width of the gap, which could be used to shape the pole itself to improve the magnetic field homogeneity. This set of optimized variables was selected to avoid interpenetration of solids during the optimization process. Similar choices of the geometric parameters were made for the other configurations.

III. Results and Discussion

Three different magnet configurations were optimized, with current densities in the coils set to either 10 A/mm^2 or 20 A/mm^2: the hourglass (HG) magnet, the windowframe (WF) magnet and the H-type (HM) magnet. In the hourglass configuration, the resistive coils are tilted but still parallel to the lateral branches of the iron yoke. In the windowframe configuration, two variants are proposed with either 1 or 3 coils, labelled as WF1 and WF3 respectively.

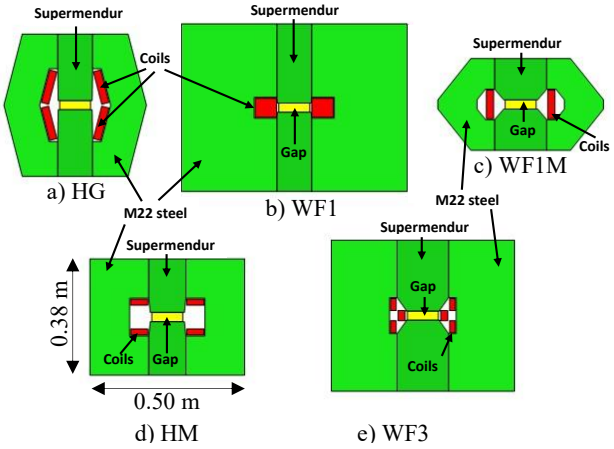

Fig. 4. Summary of the optimized geometries (figures are in scale): a) HG, J = 10 A/mm^2, E_{magn} = 5.71 kJ/m; b) WF#1, J = 10 A/mm^2, E_{magn} = 5.37 kJ/m; c) WF#1M, J = 20 A/mm^2, E_{magn} = 6.05 kJ/m; d) HM, J = 20 A/mm^2, E_{magn} = 5.74 kJ/m; e) WF#3, J = 20 A/mm^2, E_{magn} = 5.36 kJ/m.

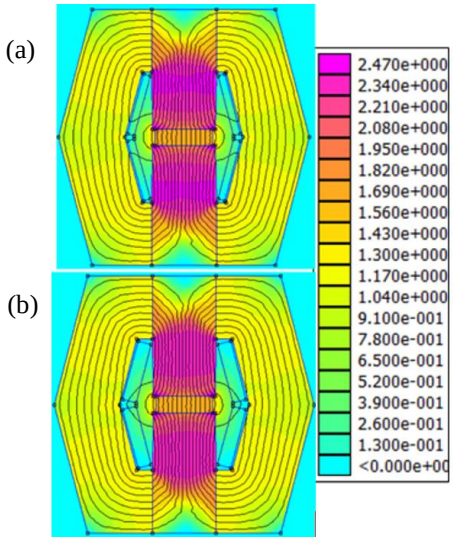

Fig. 5. Magnetic field map of the hourglass (HG) magnet geometry with a) J = 20 A/mm^2, b) J = 10 A/mm^2.

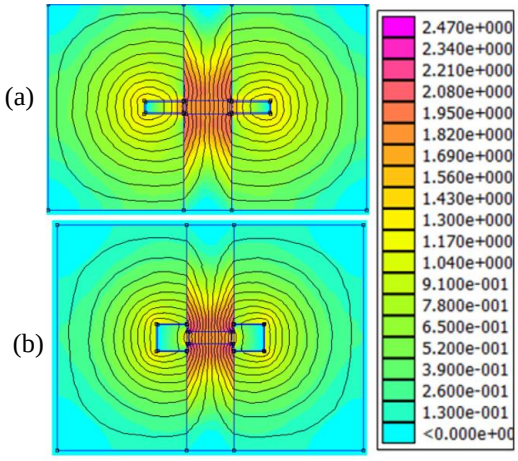

Fig. 6. Magnetic field map of the windowframe (WF1) magnet geometry with a) J = 20 A/mm^2, b) J = 10 A/mm^2.

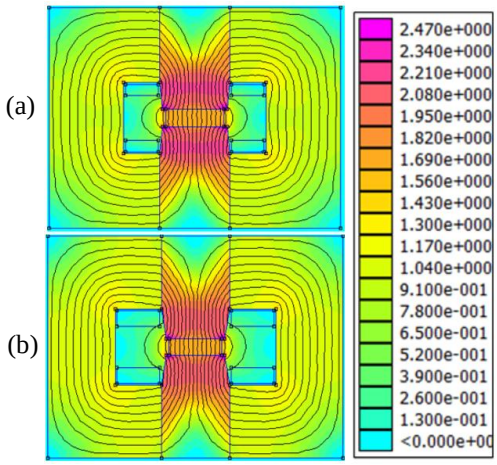

Fig. 7. Magnetic field map of the H-type (HM) magnet geometry with a) J = 20 A/mm^2, b) J = 10 A/mm^2.

A further configuration with a reduced volume of iron-yoke (WF1M) is also proposed. A summary of the optimized configurations obtained by minimizing the total energy in the magnet is shown in Fig. 4.

TABLE I
COMPARISON OF THE OPTIMIZED CONFIGURATIONS (20 A/mm^2)

		HG	WF1	WF1M	HM	WF3
DC conditions	δ_B (B_{0y} = 1.8 T)	$3.61\cdot10^{-2}$	$4.47\cdot10^{-4}$	$1.53\cdot10^{-2}$	$3.27\cdot10^{-2}$	$2.52\cdot10^{-2}$
	supermendur volume [dm^3/m]	48.2	48.7	42.9	41.3	74.0
	M22 steel volume [dm^3/m]	107.3	288.4	71.0	128.5	202.4
	copper volume [dm^3/m]	5.63	4.30	4.33	4.30	4.31
	total magnetic energy [kJ/m]	5.77	6.46	6.05	5.74	5.36
AC conditions	Imax (B_{0y} = 2 T) [kA]	23.2	47.7	48.1	23.9	15.9
	Vmax (B_{0y} = 2 T) [kV/m]	1.74	0.71	0.95	1.86	2.34
	copper losses [J/(m cycle)]	258.3	984.5	359.8	294.8	1137.5
	iron losses [J/(m cycle)]	148.1	50.4	123.4	128.1	67.7
	total loss [J/(m cycle)]	406.4	1034.9	483.2	422.9	1205.2

In Table 1, the main results of the proposed configurations – in terms of volumes, magnetic energy, copper and iron losses, magnetic field homogeneity – are compared. It can be noted that the energy lost in one cycle is thus much smaller than that required to generate the magnetic field. The losses in the copper are greater than those in the iron. It should however be noted that the AC losses in the copper were not optimized by conductor segmentation at this design stage. The field maps for the two considered values of current density are reported in figs. 5, 6, and 7 for the hourglass, windowframe and H-type magnet configurations respectively.

A. *Hourglass (HG) configuration*

In this configuration the iron yoke and the windings are both tilted with the same angle. The flux lines are therefore parallel to the conductor, thus reducing the losses in the conductor (258.3 J/(m cycle)). As shown in Figs. 5 through 7, the field in the magnetic poles found in the HG configuration is higher than that obtained with the windowframe and the H-type magnets. This results in higher iron losses (148.1 J/(m cycle)) in this configuration with respect to the others (see Table I). This magnet configuration exhibits a remarkable drawback consisting in the technical difficulty of bending the conductor at the magnet ends to manufacture the saddle coil. A total energy of 5.77 kJ/m is stored in the magnet; the energy stored in the air gap, at the specified field of 1.8 T is the same for all magnets and amounts to 3.87 kJ/m. Therefore, the energy of the gap is about 67 % of the total energy.

B. *Windowframe (WF) configuration*

The windowframe configuration was investigated with either 1 (WF1) or 3 (WF3) coils. The WF1 has the highest field uniformity ($4.47\cdot10^{-4}$), which is within the design criteria. Therefore, it does not require any shaping of the magnetic pole extremities, which is instead necessary for the other configurations. As shown in Fig. 6, the main drawback of this configuration is the large volume of the iron-yoke, that makes it impractical. To reduce the amount of iron, a modified configuration, referred to as WF1M, was examined, which eliminates the corners of the iron yoke where the magnetic field is very low (see Fig. 5). However, the stored magnetic energies in both WF1 and WF1M, 6.46 kJ/m and 6.05 kJ/m respectively, are among the highest obtained with the proposed configurations. This observation led to rule out the windowframe configuration.

C. *H-type (HM) configuration*

The HM configuration leads to low total magnetic energy (see Table I) and is thus one of the candidates for the final selection. In comparison with the HG magnet, the copper losses are higher (294.8 J/(m cycle)), since the flux lines are not parallel to the conductor, the iron losses are lower (128.1 J/(m cycle)), given the smaller intensity of the magnetic field in the poles. Moreover, the orientation of the conductor makes the manufacturing of the magnet ends easier. Finally, the position of the conductor with respect to the air gap should determine a lower beam loss effect on the conductor itself.

Due to these advantages, this configuration was selected for the following design steps.

CONCLUSION

An optimization procedure based on the minimization of the total stored energy was applied for the design of the resistive dipoles of the Rapid Cycling Synchrotrons of the Muon Collider. Three configurations were analyzed, namely the hourglass, the windowframe and the H-type magnet. All configurations reach the prescribed magnetic field in the air gap.

No configuration is optimal for all requirements (magnetic energy, losses, field homogeneity). The minimum energy found is around 5.4 kJ/m, which is reached with several design options. The configurations which exhibit the lowest energy are: WF1 (5.38 kJ/m) at 10 A/mm2 and WF3 (5.36 kJ/m) at 20 A/mm^2. These window frame configurations exhibit larger copper losses than the others, since the coils at the pole extremities are subjected to a strong flux density, but lower iron losses, given the large size of the iron yoke. The configuration exhibiting the best field homogeneity is the window frame magnet with one coil.

The best compromise between energy, losses and manufacturing simplicity leads to the choice of the H-type magnet. Further analyses will be devoted to optimizing the copper losses, the field homogeneity in the air gap and to assess whether the activation of the cobalt in the Supermendur material is acceptable in this accelerator.

REFERENCES

[1] C. Accettura *et al* "Towards a muon collider", *Eur. Phys. J. C*, vol. 83, no. 864, 2023, https://doi.org/10.1140/epjc/s10052-023-11889-x

[2] K. Long, D. Lucchesi, M. Palmer, N. Pastrone, D. Schulte, V. Shiltsev, "Muon colliders to expand frontiers of particle physics." *Nat. Phys.*, vol. 17, no. 3, 89–292, 2021. https://doi.org/10.1038/s41567-020-01130-x. arXiv:2007.15684.

[3] V. Shiltsev, F. Zimmermann, "Modern and future colliders," *Rev. Mod. Phys.*, vol. 93, 015006, 2021. https://doi.org/10.1103/RevModPhys.93.015006. arXiv:2003.09084.

[4] J. Scott Berg and Holger Witte, "Pulsed synchrotrons for very rapid acceleration", AIP Conference Proceedings 1777, 100002, 2016, https://doi.org/10.1063/1.4965683

[5] J. Tanabe, "Iron Dominated Electromagnets Design, Fabrication, Assembly and Measurements", World Scientific Publishing, Singapore, 2005.

[6] Th. Zickler, "Basic design and engineering of normal-conducting, iron-dominated electromagnets", *CERN Accelerator School CAS 2009: Specialised Course on Magnets, Bruges,* 2009, https://doi.org/10.48550/arXiv.1103.1119

[7] R. H. Byrd, J. C. Gilbert, and J. Nocedal. "A Trust Region Method Based on Interior Point Techniques for Nonlinear Programming." *Mathematical Programming*, vol. 89, no. 1, 2000, pp. 149–185, 2000.

[8] R. A. Canfield, "Quadratic Multipoint Exponential Approximation: Surrogate Model for Large-Scale Optimization." *Advances in Structural and Multidisciplinary Optimization, Springer International Publishing*, 2017, pp. 648–61, doi:10.1007/978-3-319-67988-4_49.

[9] FEMM, Finite Element Method Magnetics, https://www.femm.info.

[10] C. T. WM. McLyman, "Transformer and Inductor design handbook", Marcel Dekker, Inc, 2004.

[11] AK Steel Corporation, "Selection of Electrical Steels for Magnetic Cores", Production Data Bulletin, https://www.aksteel.eu/.